iScience

CellPress
OPEN ACCESS

Article

HOXA11 promotes lymphatic metastasis of gastric cancer via transcriptional activation of TGFβ1

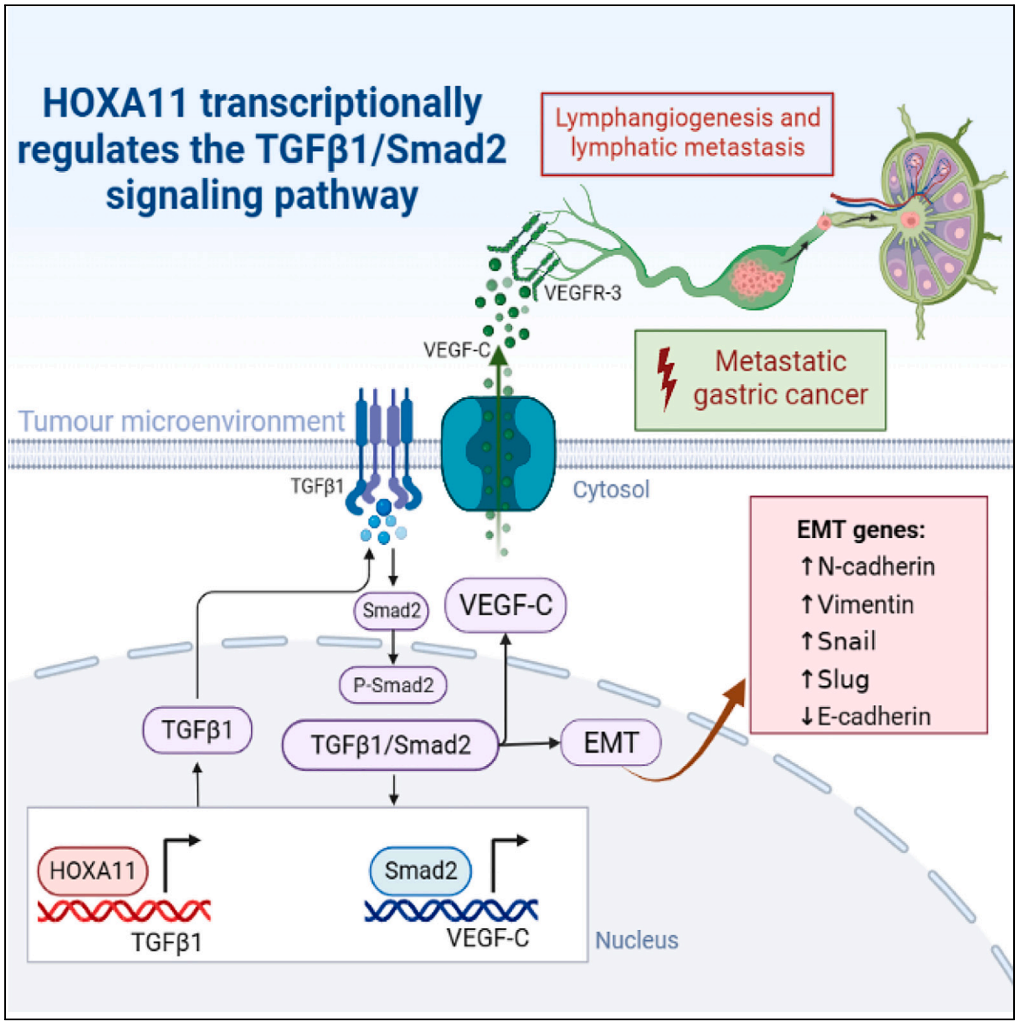

Zhenyuan Li, Tailiang Lu, Zhian Chen, ..., Yingxin Ren, Weihong Guo, Yanfeng Hu

drguowh@163.com (W.G.)
banby@smu.edu.cn (Y.H.)

Highlights

HOXA11 is highly expressed in gastric cancer and metastatic lymph nodes

HOXA11 promotes the invasion and metastasis of gastric cancer cells

HOXA11 induces the formation of tumor-associated lymphatic vessels

HOXA11 promotes EMT and lymphatic metastasis through activation of TGFβ1/Smad2 pathway

Li et al., iScience 26, 107346
August 18, 2023
https://doi.org/10.1016/j.isci.2023.107346

iScience

CellPress
OPEN ACCESS

Article

HOXA11 promotes lymphatic metastasis of gastric cancer via transcriptional activation of TGFβ1

Zhenyuan Li,[1,2] Tailiang Lu,[1,2] Zhian Chen,[1,2] Xiang Yu,[1] Lingzhi Wang,[1] Guodong Shen,[1] Huilin Huang,[1] Zhenhao Li,[1] Yingxin Ren,[1] Weihong Guo,[1,*] and Yanfeng Hu[1,3,*]

SUMMARY

Most gastric cancer (GC) patients with early stage often have no lymph node (LN) metastases, while LN metastases appear in the advanced stage. However, there are some patients who present with early stage LN metastases and no LN metastases in the advanced stage. To explore the deeper molecular mechanisms involved, we collected clinical samples from early and advanced stage GC with and without LN metastases, as well as metastatic lymph nodes. Herein, we identified a key target, HOXA11, that was upregulated in GC tissues and closely associated with lymphatic metastases. HOXA11 transcriptionally regulates TGFβ1 expression and activates the TGFβ1/Smad2 pathway, which not only promotes EMT development but also induces VEGF-C secretion and lymphangiogenesis. These findings provide a plausible mechanism for HOXA11-modulated tumor in lymphatic metastasis and suggest that HOXA11 may represent a potential therapeutic target for clinical intervention in LN-metastatic gastric cancer.

INTRODUCTION

Clinically, lymph node (LN) metastasis is one of the major factors that influences poor prognosis in gastric cancer (GC) patients.[1–3] However, some GC patients with early stage present with LN metastasis while those with advanced stage do not have LN metastasis. GC LN metastasis is an extremely complicated biological process. It involves many processes, such as tumor cell proliferation, migration, invasion, and lymphangiogenesis.[4–6] Therefore, a better understanding of the molecular mechanism underlying GC metastasis and identification of key therapeutic targets to suppress LN metastasis are urgently required for improving the survival outcomes of GC patients.

Recently, RNA-seq has transformed biomedical research, advancing the understanding of transcriptional regulatory networks and identifying diagnostic and prognostic biomarkers for many diseases.[7–9] In this study, we performed deep transcriptome sequencing followed by bioinformatic analysis of GC clinical samples with and without LN metastases at early stages, as well as with and without LN metastases at advanced stages. It revealed that the homeobox (HOX) genes family may be closely associated with LN metastasis in GC. HOX genes play a key role in cell proliferation, apoptosis, and migration. HOXA11 is a transcription factor and a member of the HOX gene family.[10–12] Previous studies have shown that HOXA11 expression is upregulated in a variety of malignancies such as breast, ovarian, endometrial, and non-small cell lung cancers, and that its high expression promotes tumor cell proliferation and is associated with poor patient prognosis.[13–16] However, the molecular mechanism of HOXA11 in GC invasion and LN metastasis has not been fully elucidated.

Epithelial-mesenchymal transition (EMT) is an important step in the process of tumor cell invasion and migration.[17] Among the multitude of different signaling molecules found in the GC, transforming growth factor β (TGFβ) is known to play an important role in the EMT effect in primary cancer. The invasive metastatic properties of tumor cells via EMT are enhanced following activation of the TGFβ signaling pathway, further making tumor cells susceptible to lymphatic metastasis.[18,19]

In addition, tumor cell-induced lymphangiogenesis is also a key step in lymphatic metastasis, where VEGF-C and VEGF-D of the vascular endothelial growth factor receptor (VEGFR) family have been reported to play an important regulatory role in lymphangiogenesis as ligands for VEGFR-3.[20,21] Accumulating evidence has revealed that VEGF-C is overexpressed and positively correlated with lymphatic vessels density

[1]Department of General Surgery, Guangdong Provincial Key Laboratory of Precision Medicine for Gastrointestinal Tumor, Nanfang Hospital, the First School of Clinical Medicine, Southern Medical University, Guangzhou 510515, P.R. China

[2]These authors contributed equally

[3]Lead contact

*Correspondence: drguowh@163.com (W.G.), banby@smu.edu.cn (Y.H.)

https://doi.org/10.1016/j.isci.2023.107346

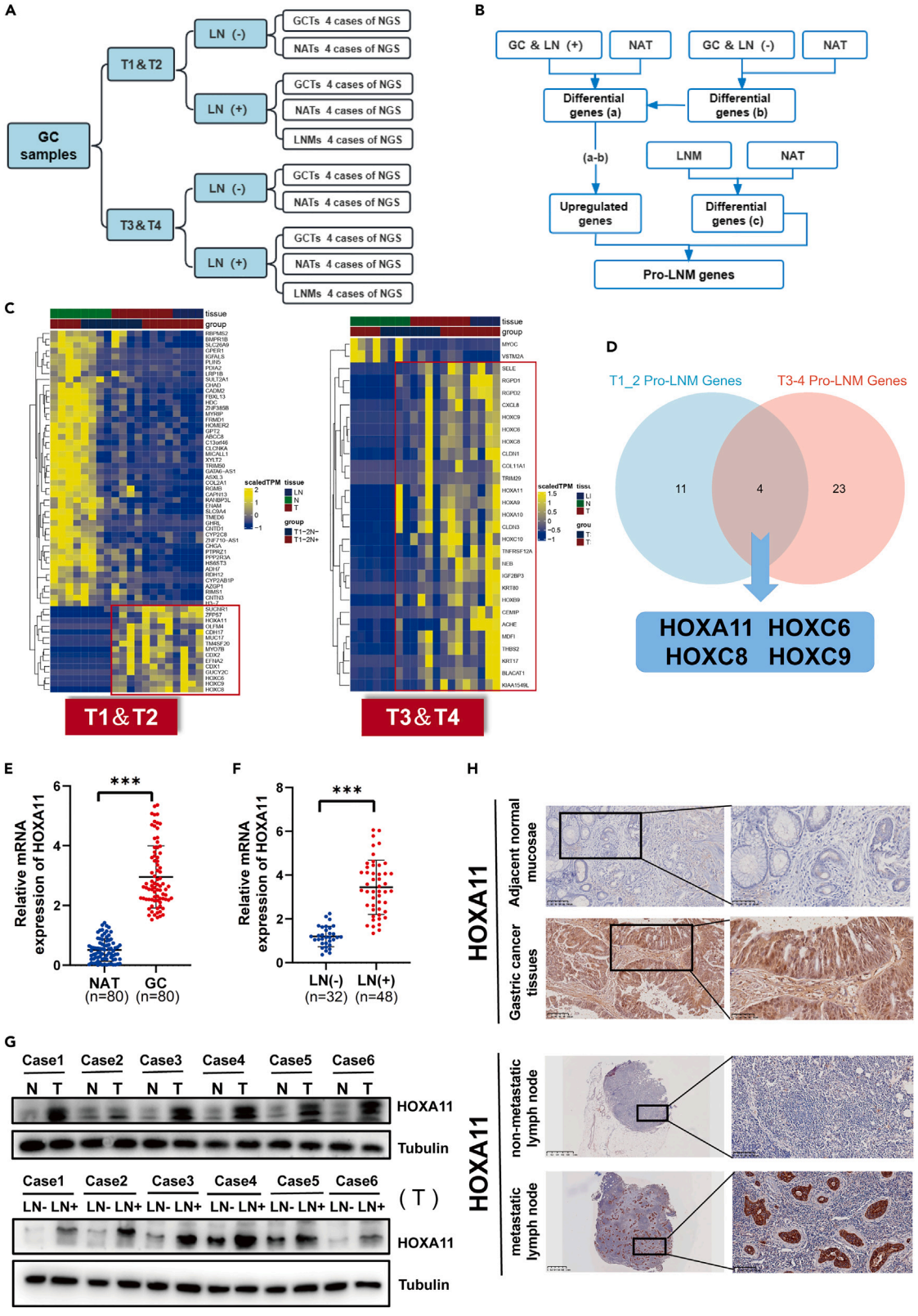
A
GC samples
T1 & T2
T3 & T4
LN (-)
LN (+)
GCTs 4 cases of NGS
NATs 4 cases of NGS
LNMs 4 cases of NGS
B
GC & LN (+)
NAT
GC & LN (-)
NAT
Differential genes (a)
Differential genes (b)
(a-b)
LNM
NAT
Upregulated genes
Differential genes (c)
Pro-LNM genes
C
tissue
group
scaledTPM
T1&T2
T3&T4
D
T1_2 Pro-LNM Genes
T3-4 Pro-LNM Genes
11
4
23
HOXA11 HOXC6
HOXC8 HOXC9
E
Relative mRNA expression of HOXA11
***
NAT (n=80)
GC (n=80)
F
Relative mRNA expression of HOXA11
***
LN(-) (n=32)
LN(+) (n=48)
G
Case1 Case2 Case3 Case4 Case5 Case6
N T
HOXA11
Tubulin
LN- LN+
(T)
H
HOXA11
Adjacent normal mucosae
Gastric cancer tissues
non-metastatic lymph node
metastatic lymph node

Figure 1. HOXA11 expression is upregulated in GC tissue and associated with LN metastasis

(A) Sample cases of NGS were collected.

(B) Schematic diagram of the analytical screening for the promotion of lymph node metastasis in gastric cancer.

(C and D) The heatmap analysis results for T1, T2 early gastric cancer group and T3, T4 advanced gastric cancer group.

(E) Expression of HOXA11 at the mRNA level in gastric cancer tissues and paired normal adjacent tissues.

(F) Comparison of mRNA levels of HOXA11 in LN-negative and LN-positive gastric cancer tissues.

(G) Expression of HOXA11 at the protein level in gastric cancer tissues and paired adjacent normal gastric mucosal tissues.

(H) Immunohistochemical results of HOXA11 in normal gastric mucosal tissue versus gastric cancer tissue and normal lymph nodes versus metastatic lymph nodes. Scale bars: 100 μm and 50 μm. The data are presented as the mean ± SEM of three independent experiments. *$p < 0.05$, **$p < 0.01$, ***$p < 0.001$.

and LN metastasis in a variety of malignancies, including breast cancer, colorectal cancer, lung cancer, and gastric cancer.[22–24] Importantly, evidence suggests that TGFβ signaling may promotes VEGF-mediated lymphangiogenesis in solid tumors.[25,26] Therefore, exploring the process that triggers lymphangiogenesis in tumors is important and far-reaching for clarifying the specific mechanism of lymphatic metastasis in GC.

In this study, we explored HOXA11 as a key target for promoting lymphatic metastasis in GC. It was demonstrated that HOXA11 activates the TGFβ1/Smad2 signaling pathway through transcriptional regulation of TGFβ1 expression. On the one hand, it could promote EMT progression and played a pro-metastatic role in GC. On the other hand, it also increased the expression and secretion of VEGF-C gene, which in turn induced the formation of lymphatic vessels, thus promoting GC invasion and lymphatic metastasis.

RESULTS

Screening for genes that promote lymph node metastasis in gastric cancer

To identify critical genes that promote LN metastasis in GC, next-generation sequencing (NGS) was performed in 16 pairs gastric cancer tissues (GCTs) and normal adjacent tissues (NATs), as well as 8 cases of metastatic lymph nodes (LNMs). As shown in Figure 1A, these clinical samples included 4 pairs of T1 and T2 early LN-negative GCTs and NATs, 4 pairs of T1 and T2 early LN-positive GCTs and NATs, and the corresponding LNMs, 4 pairs of T3 and T4 advanced LN-negative GCTs and NATs, 4 pairs of T3 and T4 advanced LN-positive GCTs and NATs, and the corresponding LNMs (Table S1).

As shown in Figure 1B, genes (a) are those that are highly expressed in differential analysis of gastric cancer with LN metastasis and its adjacent normal gastric tissue. It represents the portion of genes that are associated with gastric carcinogenesis and also with LN metastasis. Genes (b) are those that are highly expressed in differential analysis of gastric cancer without LN metastasis and its adjacent normal gastric tissue. It represents this fraction of genes that are associated with gastric carcinogenesis, but less associated with LN metastasis. Therefore, the genes we obtained by (a-b) are those that are not only associated with the development of gastric cancer, but also have a higher correlation with GC LN metastasis. Subsequently, genes (c) are those obtained from differential analysis of metastatic lymph nodes versus normal gastric tissue. It represents those that are highly expressed in metastatic LNs. Finally, the genes obtained from the genes (a-b) and genes (c) intersection analysis were those with the highest correlation with LN metastasis in GC.

In order to avoid the influence of the depth of tumor infiltration at T-stage on the results of LN metastasis analysis, we divided the GC tissues into two groups for analysis, T1-2 early stage and T3-4 progressive stage, according to the aforementioned analysis scheme. There were 15 significantly upregulated genes associated with the promotion of LN metastasis in T1 and T2 early GC tissues. In T3 and T4 advanced gastric cancer tissues, there were 27 genes that may promote LN metastasis. Comprehensive analysis revealed that four HOX family–related genes, including HOXA11, HOXC6, HOXC8, and HOXC9, were consistently upregulated in both early and advanced GC tissues with LN metastasis (Figures 1C and 1D).

Notably, quantitative real-time PCR (qRT-PCR) assay further confirmed the expression levels of four upregulated candidate HOX genes in 80 paired GC cancer tissues and matched normal tissues (Figures 1E and S1A–S1C). In contrast, comparison of GC tissues grouped as LN-positive and LN-negative revealed that only the HOXA11 target gene was significantly overexpressed, as determined by qRT-PCR analysis ($p < 0.01$, Figure 1F). In addition, statistical analysis showed that HOXA11 expression was closely associated with LN metastatic status, tumor vascular infiltration and AJCC stage in GC patients ($n = 80$; Table S2). Moreover, consistent with the qRT-PCR results, GC tissues and paired normal mucosal tissues were subjected to tissue protein extraction, followed by western blot to detect differences in HOXA11 expression. As shown in Figure 1G, we found that the protein expression level of HOXA11 was significantly higher in most of the

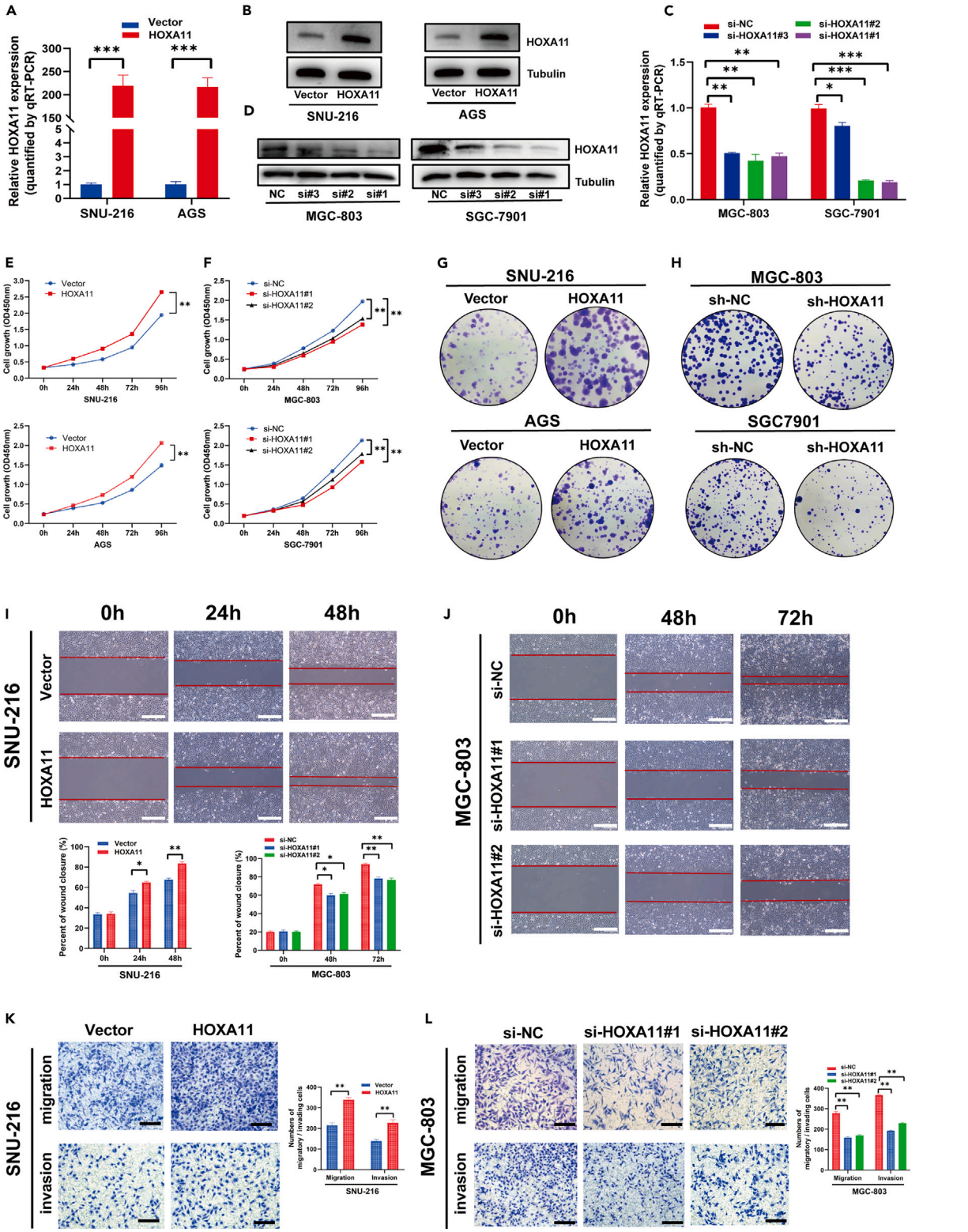

Figure 2. Overexpression of HOXA11 promotes the proliferation, migration and invasive ability of GC cells *in vitro*

(A–D) Construction of a gastric cancer cell line silencing and overexpressing HOXA11 verified by qRT-PCR and WB assays.

(E and F) The ability of HOXA11 overexpression or knockdown to affect the proliferation of gastric cancer cells *in vitro* was determined by CCK-8 assay.

Figure 2. *Continued*

(G and H) The ability of HOXA11 overexpression or knockdown to affect clone formation in gastric cancer cells *in vitro* was determined by plate clone formation assays.

(I and J) The ability of HOXA11 overexpression or knockdown to affect the migration of gastric cancer cells *in vitro* was determined by a cell scratch healing assay, Scale bar: 100 μm.

(K and L) The ability of HOXA11 overexpression or knockdown to affect the migration and invasion of gastric cancer cells *in vitro* was determined by Transwell assay, Scale bar: 100 μm. The data are presented as the mean ± SEM of three independent experiments. *$p < 0.05$, **$p < 0.01$, ***$p < 0.001$.

GC tissues than in their paired normal mucosal tissues. And the expression was higher in GC tissues with LN metastasis than in those without LN metastasis.

To further investigate the role of HOXA11 in GC progression, the HOXA11 protein expression level was examined in different gastric tissues types (n = 80) via immunohistochemical (IHC) analysis. As shown in Figure 1H, HOXA11 was lowly expressed in NAT, whereas it was significantly highly expressed in LN-positive GC tissues. More importantly, we observed that metastatic lymph nodes samples were positively stained for HOXA11. In summary, HOXA11 plays an important role in the lymphatic metastasis of GC.

Moreover, analysis of the TCGA public database revealed that HOXA11 was also highly expressed in GC. The Kaplan-Meier Plotter database showed that high HOXA11 expression predicted poor prognosis and was associated with low overall survival (OS) in GC patients ($p < 0.01$). ROC curve analysis also showed that HOXA11 expression was an independent prognostic factor in GC patients (Figures S1D–S1F).

HOXA11 promotes proliferation, migration and invasive metastasis of GC cells *in vitro*

As HOXA11 expression is upregulated in GC tissues and associated with metastasis, we subsequently investigated whether HOXA11 affects the ability of GC cells to proliferate, migrate and invade and metastasize *in vitro*. Western blot and RT-PCR assays revealed that the expression level of HOXA11 was significantly elevated in human gastric cancer cell lines MGC803 and SGC7901, which were suitable for relevant experiments to silence its expression. The relatively low expression of HOXA11 in SNU216 and AGS GC cell lines is suitable for experiments related to increasing its expression (Figures S2A and S2B). Therefore, we have successfully constructed SNU216 and AGS GC cells that stably overexpress HOXA11, as well as MGC803 and SGC7901 GC cells that interfere with HOXA11 expression (Figures 2A–2D).

First of all, the growth curves determined by CCK-8 assays showed that HOXA11 upregulation promoted SNU216 and AGS proliferation while HOXA11 downregulation significantly inhibited MGC803 and SGC7901 proliferation (Figures 2E and 2F). Similarly, clonogenic assay of cell proliferation also showed observations that are consistent with the CCK-8 assay (Figures 2G and 2H).

Furthermore, migration and invasive metastasis ability was measured by wound healing and transwell assays. As shown in Figures 2I and 2J, wound healing assays demonstrated that overexpression of HOXA11 in SNU216 and AGS cells healed significantly faster than the corresponding control cells, while interference with HOXA11 expression was relatively slower in MGC803 and SGC7901 cells. Correspondingly, the following transwell assay showed that HOXA11 overexpressing GC cells had a nearly 2-fold increase in the number of cells migrating and invading compared to the control group, while knockdown of HOXA11 expression showed an opposite trend (Figures 2K, 2L and S2C–S2E). These results suggest that HOXA11 can promote the proliferation, migration and invasive metastatic ability of GC cells *in vitro*.

HOXA11 regulates EMT through TGFβ signaling to promote gastric cancer cell metastasis

Epithelial mesenchymal transition (EMT) is an important step in the process of migration and invasive metastasis of GC cells.[27,28] As activation of the TGFβ signaling pathway can promote EMT occurrence, to verify whether HOXA11 is involved in this pathway, RT-qPCR and Western blot were used to detect key genes of this signaling pathway in GC cells after knockdown and overexpression of HOXA11.

As shown in Figures 3A–3D, the results of both RT-qPCR and western blot experiments showed that the expression of mesenchymal markers N-cadherin, Vimentin, Slug, and Snail were upregulated while the expression of epithelial marker E-cadherin was downregulated in GC cells overexpressing HOXA11. And the opposite experimental result was observed after HOXA11 interference. Also, the RNA expression levels of the three isoforms of TGFβ1, TGFβ2 and TGFβ3 in the TGFβ signaling pathway, only TGFβ1 was significantly elevated in GC cells overexpressing HOXA11 and decreased after interference with HOXA11 expression.

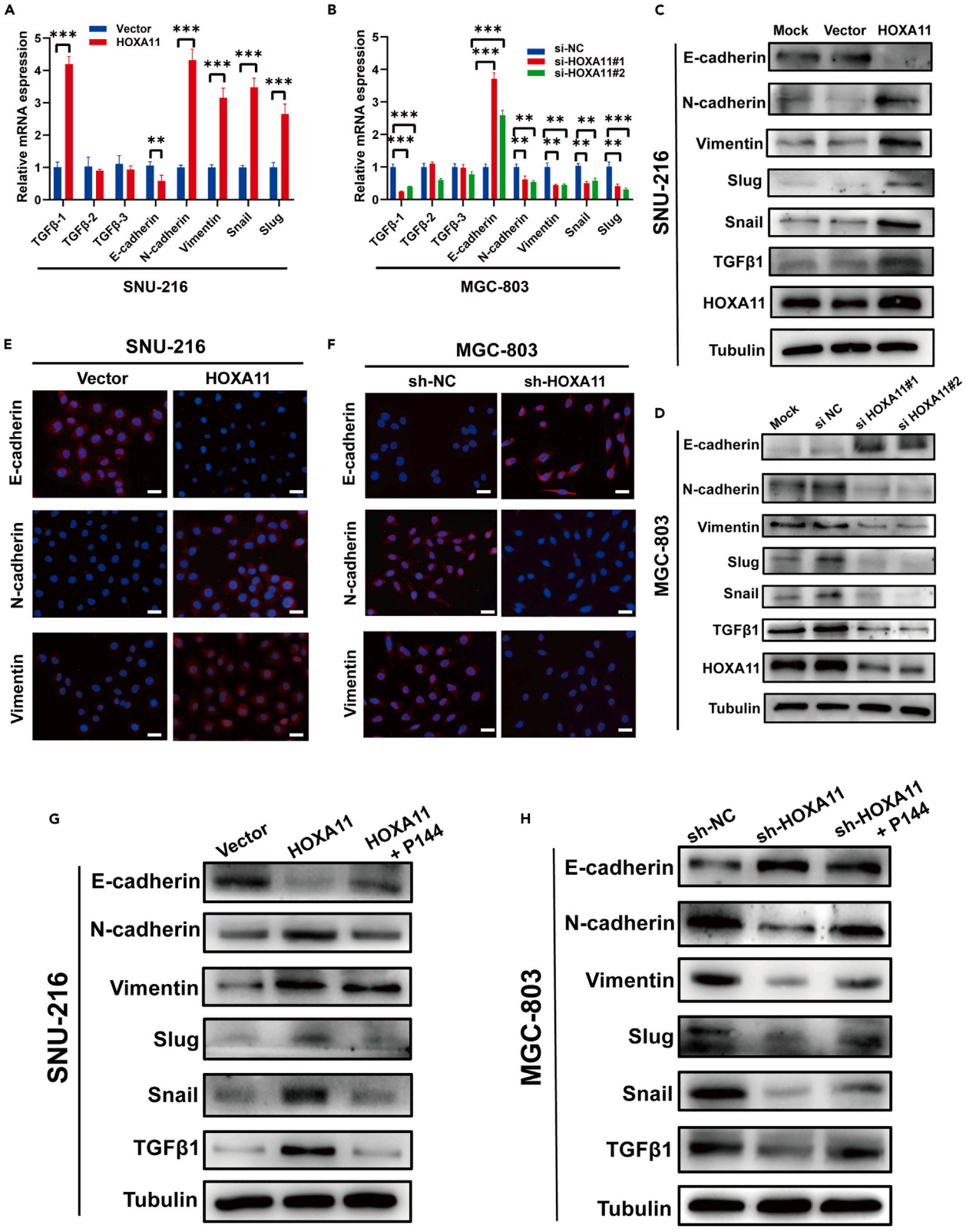
A
Vector
HOXA11
Relative mRNA espression
TGFβ-1
TGFβ-2
TGFβ-3
E-cadherin
N-cadherin
Vimentin
Snail
Slug
SNU-216
B
si-NC
si-HOXA11#1
si-HOXA11#2
Relative mRNA espression
MGC-803
C
Mock
Vector
HOXA11
SNU-216
E-cadherin
N-cadherin
Vimentin
Slug
Snail
TGFβ1
HOXA11
Tubulin
D
Mock
si NC
si HOXA11#1
si HOXA11#2
MGC-803
E-cadherin
N-cadherin
Vimentin
Slug
Snail
TGFβ1
HOXA11
Tubulin
E
SNU-216
Vector
HOXA11
E-cadherin
N-cadherin
Vimentin
F
MGC-803
sh-NC
sh-HOXA11
E-cadherin
N-cadherin
Vimentin
G
Vector
HOXA11
HOXA11 + P144
SNU-216
E-cadherin
N-cadherin
Vimentin
Slug
Snail
TGFβ1
Tubulin
H
sh-NC
sh-HOXA11
sh-HOXA11 + P144
MGC-803
E-cadherin
N-cadherin
Vimentin
Slug
Snail
TGFβ1
Tubulin

Figure 3. HOXA11 regulates EMT through TGFβ signaling to promote gastric cancer cell metastasis

(A–D) Gastric cancer cells with HOXA11 overexpression (A and C) or knockdown (B and D) affecting the expression of TGFβ signaling molecules as well as E-cadherin, N-cadherin, Vimentin, Slug and Snail key molecules in EMT were determined by RT-qPCR and western blot assays.

(E and F) The expression of E-cadherin, N-cadherin and Vimentin in gastric cancer cells affected by HOXA11 overexpression (E) or knockdown (F) was determined by cellular immunofluorescence assays, Scale bar: 20 μm.

(G and H) Protein expression of TGFβ1 and EMT key molecules was determined by treating HOXA11 overexpressed (G) or knocked down (H) gastric cancer cells with the TGFβ1 signaling pathway inhibitor P144. The data are presented as the mean ± SEM of three independent experiments. *$p < 0.05$, **$p < 0.01$, ***$p < 0.001$.

In addition, the effect of HOXA11 expression on the characteristic EMT marker was further verified by cellular immunofluorescence assays. In SNU216 and AGS cells overexpressing HOXA11, the fluorescence expression brightness of mesenchymal markers N-cadherin and Vimentin was significantly upregulated compared to the control group, while the expression of epithelial marker E-cadherin was downregulated. Similarly, in MGC803 and SGC7901 cells, which interfere with HOXA11 expression, the opposite experimental results were observed (Figures 3E, 3F, S3A and S3B). In summary, these findings suggested that HOXA11 might enhance GC cells metastasis through EMT.

Subsequently, after further treatment with the TGFβ1 signaling pathway inhibitor P144, Western blot results showed that after the inhibition of TGFβ1 expression in GC cells overexpressing HOXA11, the expression of the corresponding mesenchymal markers N-cadherin, Vimentin, Slug and Snail were also downregulated, while the expression of the epithelial marker E-cadherin was partially restored and elevated. Also, in the group of GC cells with silenced HOXA11 expression, TGFβ1 inhibitors were seen to partially revert to elevated mesenchymal markers in EMT (Figures 3G and 3H). These results demonstrate that HOXA11 regulates key genes in the TGFβ1 signaling pathway and promotes the development of EMT.

HOXA11 activates nuclear expression of Smad2 in the TGFβ/Smad signaling pathway through transcriptional regulation of TGFβ1

To further verify whether HOXA11 is involved in the transcriptional regulation of TGFβ1, experimental analysis was performed by ChIP-qPCR. Based on the predictions from the database Jaspar (http://jaspar.genereg.net/), three possible HOXA11 binding sites (P1-P3) were selected in the TGFβ1 promoter, and the corresponding primers were designed and synthesized. The results of ChIP-qPCR experiments showed that HOXA11 was highly concentrated in the P2 region and that binding was higher in the HOXA11 overexpression group of cells (Figure 4A). Subsequently, the wild-type (WT) and mutant (Mut) TGFβ1 promoter-luciferase reporter vectors were constructed and genetic testing for the dual luciferase reporter gene (DLR) was performed. As shown in Figures 4B and 4C, the HOXA11 overexpression group significantly increased TGFβ1 promoter activity after wild-type TGFβ1 co-transfection. Nevertheless, no significant changes in luciferase activity were observed after co-transfection with mutant TGFβ1. The opposite experimental results were seen in the sh-HOXA11 expression group. The aforementioned experimental results confirm that TGFβ1 is a target gene regulated by HOXA11 transcription.

Elevated phosphorylated Smad2 protein in the nucleus is thought to be a marker of TGFβ signaling activation. Therefore, to explore whether HOXA11 overexpression activated the TGFβ1/Smad2 pathway, cellular immunofluorescence assays revealed that Smad2 was significantly elevated in the nuclei of SNU216 and AGS cells in which HOXA11 was overexpressed. In contrast, in GC cells of MGC803 and SGC7901 with sh-HOXA11, Smad2 expression was more in the cytoplasm and less in the nucleus compared to the control group (Figures 4D–4G). Subsequently, the expression of Smad2 and P-Smad2 in the cells was detected by Western blot assay. As shown in Figures 4H and 4I, a significant increase in P-Smad2 expression was detected in overexpressing HOXA11 GC cells. However, protein expression of P-Smad2 was reduced when cells were treated with a TGFβ1 inhibitor P144, suggesting that HOXA11 is unable to activate the Smad pathway after TGFβ1 depletion. Similarly, P-Smad2 expression was decreased in cells with silenced HOXA11 expression, while its expression level was increased after treatment with TGFβ1 inhibitors. These experimental results suggest that overexpression of the HOXA11 activates the TGFβ1/Smad2 signaling pathway in GC.

HOXA11 overexpression in gastric cancer cell cultures promotes tube formation and migratory invasion of HLECs *in vitro*

LN metastasis from GC is a complex multi-step process, with lymphatic vessel generation and migration invasion being essential for lymphatic metastasis. As shown in Figures 5A and 5C, incubation of human lymphatic endothelial cells (HLECs) with supernatant cultures from the SNU216 and AGS cell groups

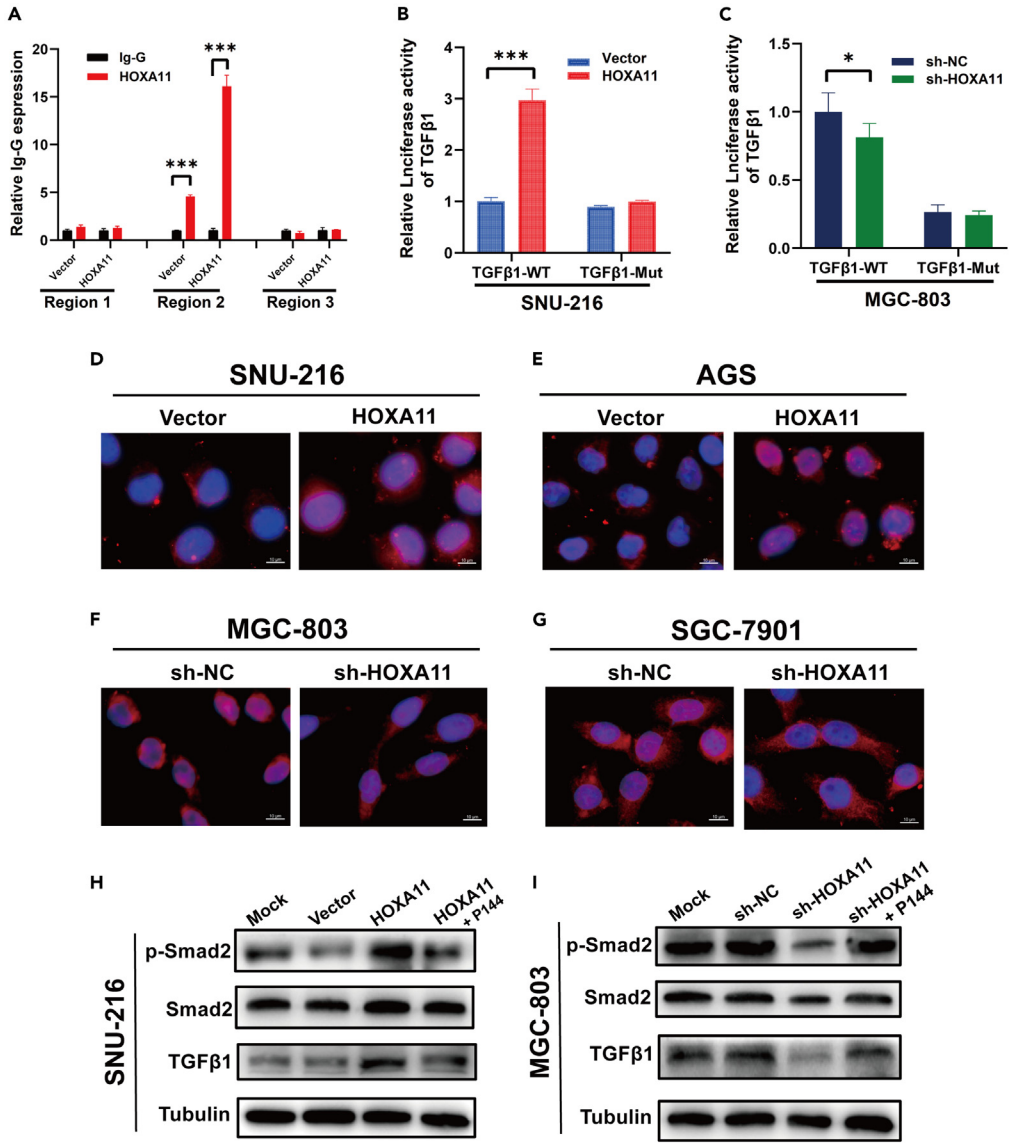

Figure 4. HOXA11 activates nuclear expression of Smad2 in the TGFβ/Smad signaling pathway through transcriptional regulation of TGFβ-1

(A) ChIP-qPCR assay revealed the potential binding sites of HOXA11 in the TGFβ1 promoter region.

(B and C) Dual-luciferase assays demonstrated that HOXA11 activated TGFβ-1 transcription through direct regulation.

(D–G) Cellular immunofluorescence assays detected Smad2 entry into the nucleus in HOXA11 overexpressed (D and E) or knockdown (F and G) gastric cancer cells, Scale bar: 10 μm.

(H and I) Western blot assays examined the protein expression of Smad-2 and P-smad2 in gastric cancer cells overexpressing (H) or knocking down (I) HOXA11 or after treatment with the TGFβ1 signaling pathway inhibitor. The data are presented as the mean ± SEM of three independent experiments. *$p < 0.05$, **$p < 0.01$, ***$p < 0.001$.

overexpressing HOXA11 was more effective in tube formation, with a nearly 2-fold increase relative to the control group. In contrast, HLECs incubated with supernatant cultures from the MGC803 and SGC7901 cell groups that interfered with HOXA11 expression had difficulty aggregating into tubes. Subsequently, relevant reversion experiments were performed by the TGFβ1 pathway inhibitor P144. The experimental results showed that the tube-forming ability of HLECs was reduced in the cell culture supernatant after the addition of P144 to the overexpression of HOXA11 cells compared to the control group. In contrast, the addition of P144-treated cell supernatant cultures to MGC803 and SGC7901 cells of sh-HOXA11 resulted in increased lymphatic vessel formation.

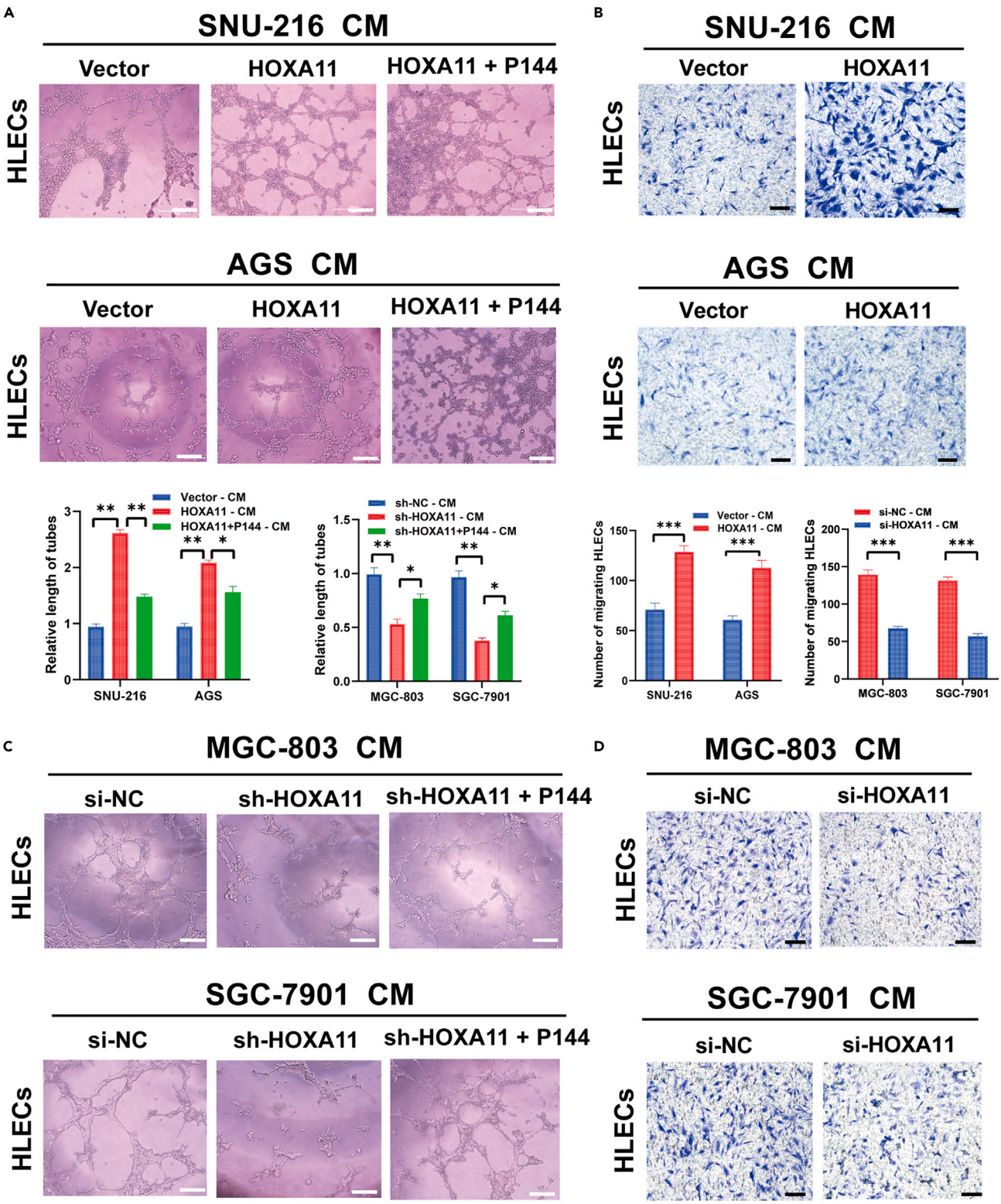
A
SNU-216 CM
Vector
HOXA11
HOXA11 + P144
HLECs
AGS CM
Vector
HOXA11
HOXA11 + P144
HLECs
Vector - CM
HOXA11 - CM
HOXA11+P144 - CM
Relative length of tubes
SNU-216
AGS
sh-NC - CM
sh-HOXA11 - CM
sh-HOXA11+P144 - CM
Relative length of tubes
MGC-803
SGC-7901
B
SNU-216 CM
Vector
HOXA11
HLECs
AGS CM
Vector
HOXA11
HLECs
Vector - CM
HOXA11 - CM
Number of migrating HLECs
SNU-216
AGS
si-NC - CM
si-HOXA11 - CM
Number of migrating HLECs
MGC-803
SGC-7901
C
MGC-803 CM
si-NC
sh-HOXA11
sh-HOXA11 + P144
HLECs
SGC-7901 CM
si-NC
sh-HOXA11
sh-HOXA11 + P144
HLECs
D
MGC-803 CM
si-NC
si-HOXA11
HLECs
SGC-7901 CM
si-NC
si-HOXA11
HLECs

Figure 5. HOXA11 overexpression in gastric cancer cell cultures promotes tube formation and migratory invasion of HLECs *in vitro*

(A and C) The ability of HOXA11 overexpression (A) or knockdown (C) of cell supernatant cultures to affect the tube-forming capacity of human lymphatic endothelial cells *in vitro* was determined by lymphatic tube formation assays, Scale bar: 100 μm.

(B and D) The ability of HOXA11 overexpression (B) or knockdown (D) of cell supernatant cultures to affect the invasive migratory capacity of human lymphatic endothelial cells *in vitro* was determined by Transwell assays, Scale bar: 100 μm. The data are presented as the mean ± SEM of three independent experiments. *$p < 0.05$, **$p < 0.01$, ***$p < 0.001$.

In addition, Transwell experiments demonstrated that cell cultures overexpressing HOXA11 treated as a chemotactic effect in the lower chamber had more HLECs able to cross the bottom membrane of the chamber, whereas the opposite was true for interference with HOXA11 expression (Figures 5B and 5D). Taken together, HOXA11 promotes invasive metastasis and tube-forming ability of lymphatic vessel endothelial cells. And the TGFβ1 signaling pathway plays a key role in HOXA11 in regulating the invasion and metastasis of GC cells, as well as promoting the expression and secretion of lymphovascular neoplastic factors.

HOXA11 promotes VEGF-C expression and secretion through activation of the TGFβ1/SMAD2 pathway

Actually, our experimental explorations revealed that HOXA11 promotes the expression and secretion of factors associated with lymphatic vessel formation, but what the exact molecular mechanism is unclear. First, vascular endothelial growth factor (VEGF) genes have been shown to promote lymphatic metastasis in a variety of tumors by inducing lymphatic vessel neogenesis and increasing lymphatic vessel density within the tumor.[5,29] Related studies have also shown that the TGFβ/SMAD signaling pathway plays an important role in the expression and secretion of VEGF-C and VEGF-D factors that promote lymphatic vessel formation.[25,30] In the present experimental results, HOXA11 significantly activated TGFβ1/SMAD2 signaling pathway. Subsequently, as shown in Figures 6A–6D, the expression of VEGF-C induced by the TGFβ1 signaling pathway was significantly higher in the overexpression of HOXA11 GC cells than in the control group by RT-qPCR and western blot assays. However, the expression of VEGF-D did not change significantly. Similar results were demonstrated in sh-HOXA11 in MGC803 and SGC7901 cells.

In addition, the main mechanism of action of VEGF-C is to secrete extracellularly and bind to the VEGF receptor to transduce cascade signals and thereby promote lymphatic vessel neogenesis.[31] Therefore, the expression of secretory VEGF-C in the conditioned medium of GC cells was examined by ELISA assay. It was found that overexpression of HOXA11 significantly upregulated secretory VEGF-C levels in cell cultures, while knockdown of HOXA11 downregulated VEGF-C levels in cell cultures (Figures 6E and 6F).

To further explore how HOXA11 activates VEGF-C expression and secretion through the TGFβ1/Smad2 signaling pathway. Following TGFβ1 stimulation, does the Smad2 key factor in the pathway, which is also an important transcription factor, bind to the promoter of VEGF-C and thus fulfill the relevant transcriptional regulatory role. Based on the predictions of the JASPAR transcription factor database, three possible Smad2 binding sites were selected on the VEGF-C promoter, and the corresponding primers were designed and synthesized. Then, the results of ChIP-qPCR experiments showed that Smad2 was significantly enhanced at multiple binding sites of VEGF-C. Moreover, Smad2 binding to the VEGF-C promoter was stronger in overexpressing HOXA11 GC cells (Figure 6G). In conclusion, these results suggest that HOXA11 enhances TGFβ1 expression, induces Smad2 activation and acts synergistically with Smad2 signaling pathway to promote VEGF-C expression and secretion, which in turn induces lymphatic vessel neogenesis and promotes lymphatic metastasis in GC.

HOXA11 promotes lymphatic metastasis *in vivo*

To further determine the role of HOXA11 in the lymphatic metastasis of GC, its LN metastasis model was constructed by loading tumor cells in the foot pad of nude mice. Lymphatic drainage from the footpad is directed toward the popliteal LNs and then the inguinal LNs. In addition, quantitative injection of footpad lymphatic drainage allows for more sensitive and accurate measurement of LN metastasis models *in vivo*.

Firstly, SNU216 GC cells with high stable HOXA11 expression and their control cells, as well as MGC803 GC cells with silent HOXA11 expression and their control cells were inoculated into the foot pads of nude mice in each group. After one month of rearing under common environmental conditions, the size of the tumors in each group was observed and the effect of HOXA11 on lymphatic metastasis was examined. Notably, the group with overexpressed HOXA11 exhibited an increased capacity for GC cell proliferation and metastasis to the LNs, as determined by the intensity of live imaging fluorescence, and fluorescence imaging of inguinal LNs could

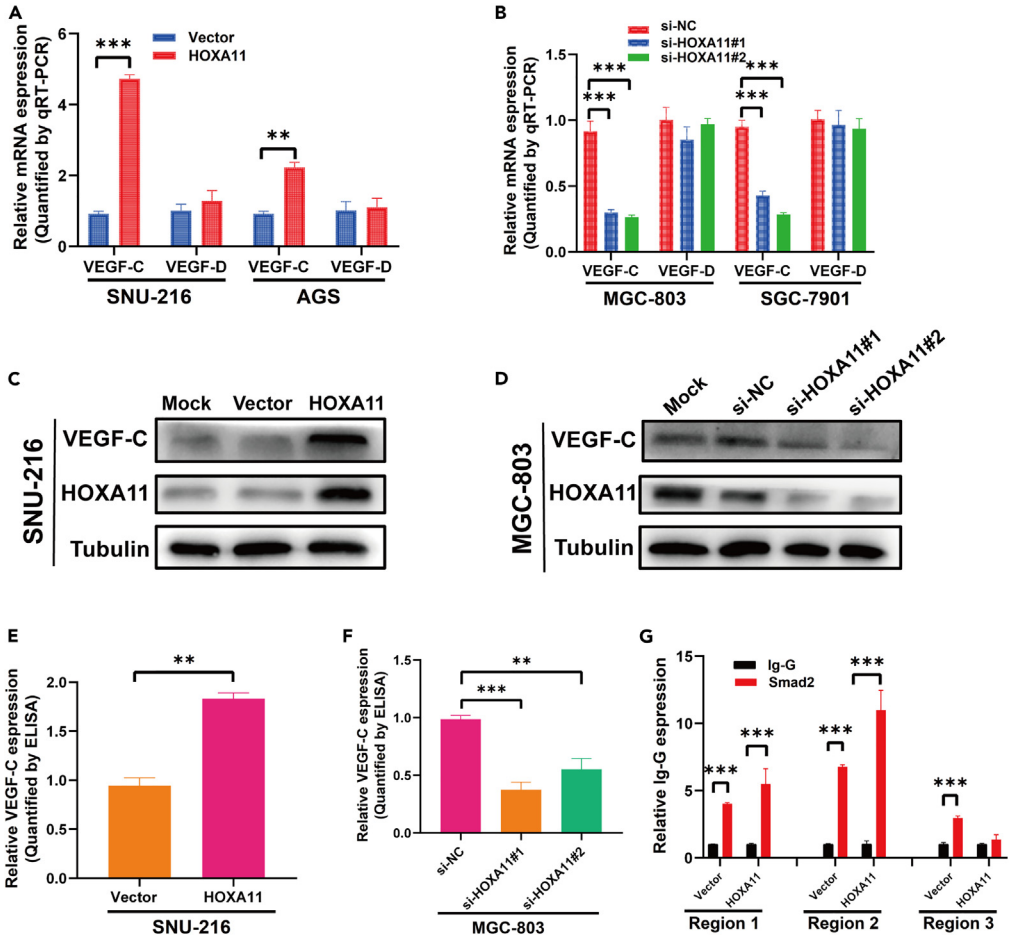

Figure 6. HOXA11 promotes VEGF-C expression and secretion through activation of the TGFβ1/SMAD2 pathway

(A–D) Expression of VEGF-C and VEGF-D in gastric cancer cells affected by HOXA11 overexpression (A and C) or knockdown (B and D) was determined by RT-qPCR and Western blot assays.

(E and F) ELISA assays determined VEGF-C expression in supernatant cultures of gastric cancer cells with HOXA11 overexpression (E) or knockdown (F).

(G) ChIP-qPCR assay revealed the potential binding sites of Smad2 in the VEGF-C promoter region. The data are presented as the mean ± SEM of three independent experiments. *p < 0.05, **p < 0.01, ***p < 0.001.

be seen (Figure 7A). The volume of primary footpad tumors and metastatic LNs in the HOXA11 overexpression group was significantly larger than that in the control group, as observed by anatomical experiments (Figures 7B and 7C). Then, as shown in Figure 7D, immunohistochemical staining (IHC) experiments showed that the lymphatic vascular neoplastic marker LYVE-1 stained more extensively and more intensely in the footpad tumors formed in the overexpression HOXA11 group compared to the control group. Enhanced expression of human pan-cytokeratin protein was also evident in the inguinal LNs, suggesting metastasis in the LNs.

In contrast, the fluorescence intensity of live imaging of nude mice in the sh-HOXA11 group was significantly weaker than that of the blank control group (Figure 7E). And the volume of primary foot pad tumor and LNs in the sh-HOXA11 group was also significantly smaller than that of the control group (Figure 7F). The aforementioned experimental results suggest that overexpression of HOXA11 contributes to the proliferation and LN metastasis of GC cells *in vivo*.

DISCUSSION

LN metastasis confers a poor prognosis on GC patients and currently has limited treatment options in the clinic.[32–34] Thus, investigations of the molecular mechanisms underlying LN metastasis and the

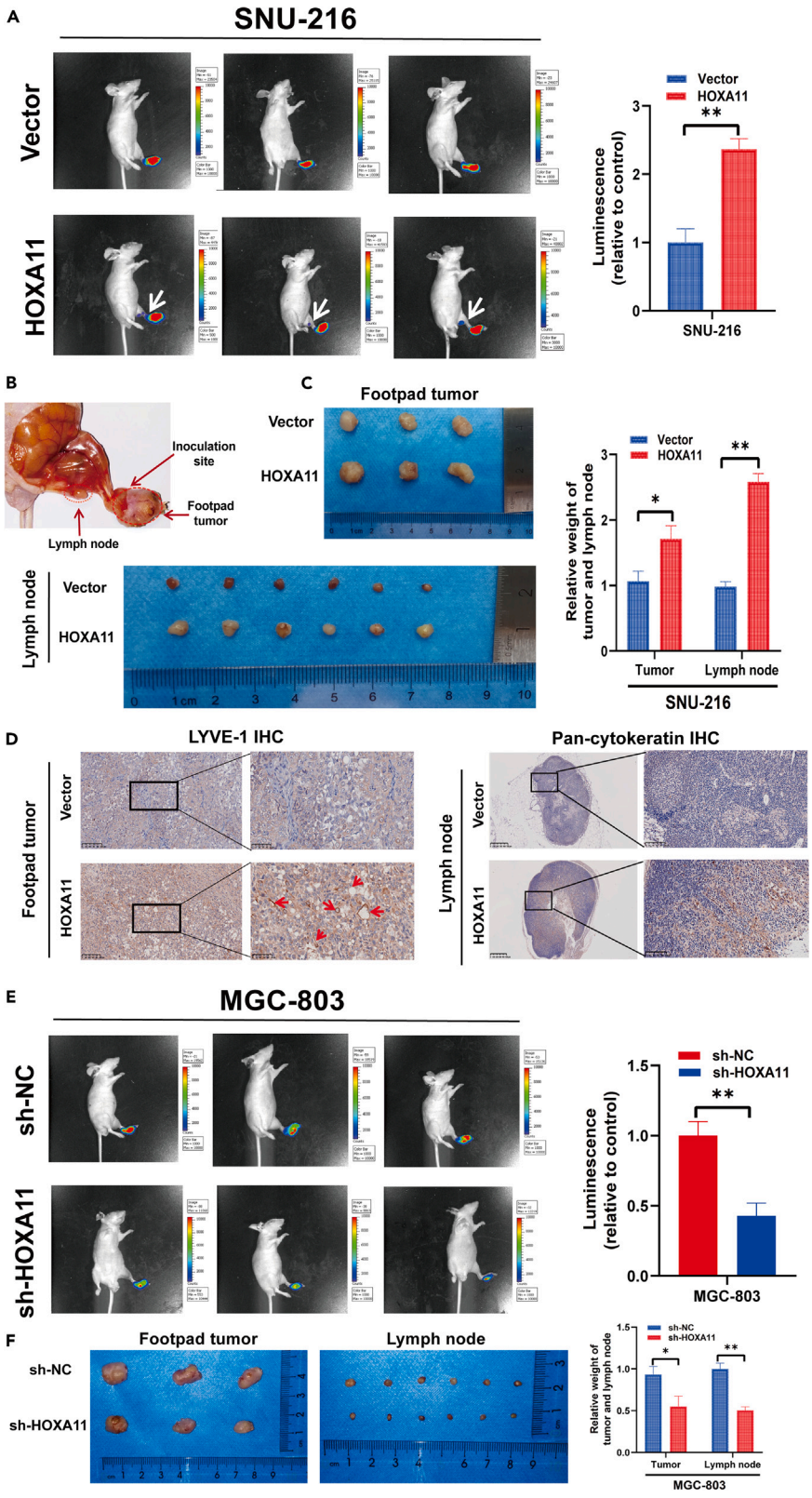
A
SNU-216
Vector
HOXA11
Vector
HOXA11
**
Luminescence (relative to control)
SNU-216
B
Inoculation site
Footpad tumor
Lymph node
C
Footpad tumor
Vector
HOXA11
Lymph node
Vector
HOXA11
Vector
HOXA11
*
**
Relative weight of tumor and lymph node
Tumor
Lymph node
SNU-216
D
LYVE-1 IHC
Pan-cytokeratin IHC
Footpad tumor
Vector
HOXA11
Lymph node
Vector
HOXA11
E
MGC-803
sh-NC
sh-HOXA11
sh-NC
sh-HOXA11
**
Luminescence (relative to control)
MGC-803
F
Footpad tumor
Lymph node
sh-NC
sh-HOXA11
sh-NC
sh-HOXA11
*
**
Relative weight of tumor and lymph node
Tumor
Lymph node
MGC-803

Figure 7. Overexpression of HOXA11 promotes tumorigenic and lymph node metastatic capacity of gastric cancer cells *in vivo*

(A) Comparison of fluorescence brightness between gastric cancer cells overexpressing HOXA11 and blank controls as measured by small animal live imaging.

(B) Representative images of a nude mouse model of footpad tumor formation and popliteal-inguinal LN metastasis.

(C) Comparison of primary tumor and popliteal-inguinal LN between gastric cancer cells overexpressing HOXA11 and blank controls as determined by animal dissection.

(D) Comparison of the expression of the lymphovascular neoplastic marker LYVE-1 in the primary tumor and the expression of the tumor metastasis marker pan-cytokeratin protein in the popliteal-inguinal LN between gastric cancer cells overexpressing HOXA11 and blank controls, as determined by immunohistochemistry. Scale bars: 100 μm and 50 μm.

(E and F) Comparison of fluorescence brightness and primary tumor with popliteal-inguinal LN between gastric cancer cells with knockdown HOXA11 and blank controls as determined by animal live imaging and dissection isolation. The data are presented as the mean ± SEM of three independent experiments. *$p < 0.05$, **$p < 0.01$, ***$p < 0.001$.

identification of novel, promising targets are urgently needed for prevention and therapy. In this study, we collected clinical GC and metastatic lymph node tissue samples and analyzed their mRNA expression profiles by second-generation sequencing technology to find molecular markers that were highly expressed in both LN-positive metastatic GC and LN tissue with metastasis.

The transcription factor HOXA11 is a member of the HOX gene family and plays an important role in transcriptional regulation. In previous studies, HOXA11 expression was reported to be upregulated in a variety of malignancies such as endometrial, ovarian, and breast cancers.[35–37] It has also been shown that overexpression of HOXA11 promotes the stemness and thus the peritoneal metastatic process of GC.[38,39] However, the role of HOXA11 in the development of GC and lymphatic metastasis remains unclear.

Herein, the correlation between HOXA11 expression levels and pathological features was validated through public databases and clinical tissue specimens. The study confirmed that HOXA11 was expressed at elevated levels in GC cells and tissue samples, and that it also be associated with LN metastasis in GC. Through *in vivo* and *in vitro* functional assays, overexpression of HOXA11 clearly plays an important role in promoting the migration invasion and lymphatic metastasis of GC cells, suggesting that HOXA11 may be a key predictive target for identifying GC progression and lymphatic metastasis.

The lymphatic metastasis of GC is a multifactorial and multi-step process that develops gradually.[40] Activation of the TGFβ signaling pathway and EMT are important steps in this process. Related studies have shown that activation of the TGFβ signaling pathway can promote the development of EMT.[41–43] In this study, the expression of mesenchymal markers such as N-cadherin, Vimentin, Slug, and Snail could be detected as significantly up-regulated in GC cells overexpressing HOXA11, while the expression of the epithelial marker E-cadherin was down-regulated. In this process, GC cells lose their epithelial properties and acquire the metastatic properties of mesenchymal cells, detaching themselves more easily from the original cancer focus and enhancing their ability to migrate and invade and metastasize.

Furthermore, Tumor-induced VEGF-C plays a crucial role in lymphangiogenesis, which is a rate-limiting step for the LN metastasis of cancer.[44–46] However, the precise mechanism is largely unknown. Studies have shown that transcription factors are a class of key molecules with specific structures that bind specifically to the promoter regions of target genes and then act as transcriptional regulators of downstream gene expression.[47,48] By exploring the molecular mechanism of the transcription factor HOXA11, we found that it has a transcriptional role in regulating TGFβ1 and activating the TGFβ1/Smad2 signaling pathway. On the one hand, it acts as a promoter of EMT, which enhances the invasive metastatic properties of GC cells. On the other hand, the activation of this signaling pathway increases the expression and secretion of the downstream VEGF-C gene, which induces the effect of lymphatic vessel neoformation. Ultimately, this dual effect leads to the development of lymphatic metastasis in GC.

Collectively, our study showed that HOXA11 transcriptionally regulates the action of TGFβ1, accelerates the invasive metastatic properties of GC cells and induces lymphangiogenesis to promote lymphatic metastasis in GC. Therefore, HOXA11 might serve as a potential predictive biomarker and therapeutic target for metastatic GC.

Limitations of the study

In this study, a popliteal LN metastasis model, in which GC cells were injected into the footpad of a mouse was used. Although footpad injection is the sensitive and quantitative method of measuring lymphatic metastasis *in vivo*, there are multiple limitations to this model. Most importantly, the microenvironment of the footpads is quite different from that of the gastric. And the role of HOXA11 in promoting lymphangiogenesis by affecting changes in other cellular components of the tumor microenvironment needs to be further investigated.

STAR★METHODS

Detailed methods are provided in the online version of this paper and include the following:

- KEY RESOURCES TABLE
- RESOURCE AVAILABILITY
  - Lead contact
  - Materials availability
  - Data and code availability
- EXPERIMENTAL MODEL AND STUDY PARTICIPANT DETAILS
  - Patients and clinical specimens
  - Cell lines and cell culture
  - Popliteal lymphatic metastasis model
- METHOD DETAILS
  - siRNA and lentiviral transduction
  - Quantitative Real Time PCR (qRT-PCR)
  - Western blot analysis
  - Immunohistochemical (IHC) staining
  - CCK-8 assay
  - Colony-forming assay
  - Cell scratch wound-healing assay
  - Cell transwell migration and invasion assays
  - HLECs tube formation assay
  - ELISA assay
  - Cellular immunofluorescence assay
  - Chromatin immunoprecipitation (ChIP)
  - Dual-luciferase reporter gene assay
- QUANTIFICATION AND STATISTICAL ANALYSIS

SUPPLEMENTAL INFORMATION

Supplemental information can be found online at https://doi.org/10.1016/j.isci.2023.107346.

ACKNOWLEDGMENTS

This work was supported by grants from National Natural Science Foundation of China (82272062), Science and Technology projects in Guangzhou (2023B03J0277), National Natural Science Foundation of China (82001948), Outstanding Youths Development Scheme of Nanfang Hospital, Southern Medical University (2022J004).

AUTHOR CONTRIBUTIONS

Y.F.H., Z.Y.L., and W.H.G. participated in the design of the study. Z.Y.L., T.L.L., Z.A.C., X.Y., L.Z.W., and Y.X.R. performed experiments and collected data. Z.Y.L. and T.L.L. performed bioinformatics analysis. Z.Y.L., G.D.S., and Z.H.L built the animal model. Z.Y.L., T.L.L., Z.A.C., L.Z.W., and H.L.H. participated in the data analysis. Z.Y.L., Y.F.H., Z.A.C., and X.Y. helped to draft the manuscript. All authors read and approved the final manuscript.

DECLARATION OF INTERESTS

The authors declare no competing interests.

INCLUSION AND DIVERSITY

We worked to ensure diversity in experimental samples through the selection of the cell lines. We support inclusive, diverse, and equitable conduct of research.

Received: May 13, 2023
Revised: June 9, 2023
Accepted: July 6, 2023
Published: July 13, 2023

REFERENCES

1. Wong, M.C.S., Huang, J., Chan, P.S.F., Choi, P., Lao, X.Q., Chan, S.M., Teoh, A., and Liang, P. (2021). Global incidence and mortality of gastric cancer, 1980-2018. JAMA Netw. Open *4*, e2118457.

2. Klein, C.A. (2020). Cancer progression and the invisible phase of metastatic colonization. Nat. Rev. Cancer *20*, 681–694.

3. Smyth, E.C., Nilsson, M., Grabsch, H.I., van Grieken, N.C., and Lordick, F. (2020). Gastric cancer. Lancet *396*, 635–648.

4. Cao, Y. (2005). Opinion: emerging mechanisms of tumour lymphangiogenesis and lymphatic metastasis. Nat. Rev. Cancer *5*, 735–743.

5. Karaman, S., and Detmar, M. (2014). Mechanisms of lymphatic metastasis. J. Clin. Invest. *124*, 922–928.

6. Stacker, S.A., Williams, S.P., Karnezis, T., Shayan, R., Fox, S.B., and Achen, M.G. (2014). Lymphangiogenesis and lymphatic vessel remodelling in cancer. Nat. Rev. Cancer *14*, 159–172.

7. Kamps, R., Brandão, R.D., Bosch, B.J.v.d., Paulussen, A.D.C., Xanthoulea, S., Blok, M.J., and Romano, A. (2017). Next-generation sequencing in oncology: genetic diagnosis, risk prediction and cancer classification. Int. J. Mol. Sci. *18*, 308.

8. Moradi, N., Ohadian Moghadam, S., and Heidarzadeh, S. (2022). Application of next-generation sequencing in the diagnosis of gastric cancer. Scand. J. Gastroenterol. *57*, 842–855.

9. Van Trappen, P.O., and Pepper, M.S. (2001). Lymphangiogenesis and lymph node microdissemination. Gynecol. Oncol. *82*, 1–3.

10. Hobert, O., and Westphal, H. (2000). Functions of LIM-homeobox genes. Trends Genet. *16*, 75–83.

11. Garcia-Fernàndez, J. (2005). The genesis and evolution of homeobox gene clusters. Nat. Rev. Genet. *6*, 881–892.

12. Castronovo, V., Kusaka, M., Chariot, A., Gielen, J., and Sobel, M. (1994). Homeobox genes: potential candidates for the transcriptional control of the transformed and invasive phenotype. Biochem. Pharmacol. *47*, 137–143.

13. Sun, Y., Zeng, C., Gan, S., Li, H., Cheng, Y., Chen, D., Li, R., and Zhu, W. (2018). LncRNA HOTTIP-mediated HOXA11 expression promotes cell growth, migration and inhibits cell apoptosis in breast cancer. Int. J. Mol. Sci. *19*, 472.

14. Hwang, J.A., Lee, B.B., Kim, Y., Park, S.E., Heo, K., Hong, S.H., Kim, Y.H., Han, J., Shim, Y.M., Lee, Y.S., et al. (2013). HOXA11 hypermethylation is associated with progression of non-small cell lung cancer. Oncotarget *4*, 2317–2325.

15. Whitcomb, B.P., Mutch, D.G., Herzog, T.J., Rader, J.S., Gibb, R.K., and Goodfellow, P.J. (2003). Frequent HOXA11 and THBS2 promoter methylation, and a methylator phenotype in endometrial adenocarcinoma. Clin. Cancer Res. *9*, 2277–2287.

16. Fiegl, H., Windbichler, G., Mueller-Holzner, E., Goebel, G., Lechner, M., Jacobs, I.J., and Widschwendter, M. (2008). HOXA11 DNA methylation–a novel prognostic biomarker in ovarian cancer. Int. J. Cancer *123*, 725–729.

17. Pastushenko, I., and Blanpain, C. (2019). EMT transition states during tumor progression and metastasis. Trends Cell Biol. *29*, 212–226.

18. Li, L., Liu, J., Xue, H., Li, C., Liu, Q., Zhou, Y., Wang, T., Wang, H., Qian, H., and Wen, T. (2020). A TGF-β-MTA1-SOX4-EZH2 signaling axis drives epithelial-mesenchymal transition in tumor metastasis. Oncogene *39*, 2125–2139.

19. Davis, F.M., Stewart, T.A., Thompson, E.W., and Monteith, G.R. (2014). Targeting EMT in cancer: opportunities for pharmacological intervention. Trends Pharmacol. Sci. *35*, 479–488.

20. Wissmann, C., and Detmar, M. (2006). Pathways targeting tumor lymphangiogenesis. Clin. Cancer Res. *12*, 6865–6868.

21. Chen, J.C., Chang, Y.W., Hong, C.C., Yu, Y.H., and Su, J.L. (2012). The role of the VEGF-C/VEGFRs axis in tumor progression and therapy. Int. J. Mol. Sci. *14*, 88–107.

22. Skobe, M., Hawighorst, T., Jackson, D.G., Prevo, R., Janes, L., Velasco, P., Riccardi, L., Alitalo, K., Claffey, K., and Detmar, M. (2001). Induction of tumor lymphangiogenesis by VEGF-C promotes breast cancer metastasis. Nat. Med. *7*, 192–198.

23. Onogawa, S., Kitadai, Y., Tanaka, S., Kuwai, T., Kuroda, T., and Chayama, K. (2004). Regulation of vascular endothelial growth factor (VEGF)-C and VEGF-D expression by the organ microenvironment in human colon carcinoma. Eur. J. Cancer *40*, 1604–1609.

24. Onogawa, S., Kitadai, Y., Tanaka, S., Kuwai, T., Kimura, S., and Chayama, K. (2004). Expression of VEGF-C and VEGF-D at the invasive edge correlates with lymph node metastasis and prognosis of patients with colorectal carcinoma. Cancer Sci. *95*, 32–39.

25. Liu, D., Li, L., Zhang, X.X., Wan, D.Y., Xi, B.X., Hu, Z., Ding, W.C., Zhu, D., Wang, X.L., Wang, W., et al. (2014). SIX1 promotes tumor lymphangiogenesis by coordinating TGFβ signals that increase expression of VEGF-C. Cancer Res. *74*, 5597–5607.

26. Pak, K.H., Park, K.C., and Cheong, J.H. (2019). VEGF-C induced by TGF- β1 signaling in gastric cancer enhances tumor-induced lymphangiogenesis. BMC Cancer *19*, 799.

27. Peng, Z., Wang, C.X., Fang, E.H., Wang, G.B., and Tong, Q. (2014). Role of epithelial-mesenchymal transition in gastric cancer initiation and progression. World J. Gastroenterol. *20*, 5403–5410.

28. Li, T., Huang, H., Shi, G., Zhao, L., Li, T., Zhang, Z., Liu, R., Hu, Y., Liu, H., Yu, J., et al. (2018). TGF-β1-SOX9 axis-inducible COL10A1 promotes invasion and metastasis in gastric cancer via epithelial-to-mesenchymal transition. Cell Death Dis. *9*, 849.

29. Saharinen, P., Eklund, L., Pulkki, K., Bono, P., and Alitalo, K. (2011). VEGF and angiopoietin signaling in tumor angiogenesis and metastasis. Trends Mol. Med. *17*, 347–362.

30. Zhu, J., Luo, Y., Zhao, Y., Kong, Y., Zheng, H., Li, Y., Gao, B., Ai, L., Huang, H., Huang, J., et al. (2021). circEHBP1 promotes lymphangiogenesis and lymphatic metastasis of bladder cancer via miR-130a-3p/TGFβR1/VEGF-D signaling. Mol. Ther. *29*, 1838–1852.

31. Su, J.L., Yen, C.J., Chen, P.S., Chuang, S.E., Hong, C.C., Kuo, I.H., Chen, H.Y., Hung, M.C., and Kuo, M.L. (2007). The role of the VEGF-C/VEGFR-3 axis in cancer progression. Br. J. Cancer *96*, 541–545.

32. Hölscher, A.H., Drebber, U., Mönig, S.P., Schulte, C., Vallböhmer, D., and Bollschweiler, E. (2009). Early gastric cancer: lymph node metastasis starts with deep mucosal infiltration. Ann. Surg. *250*, 791–797.

33. Quail, D.F., and Joyce, J.A. (2013). Microenvironmental regulation of tumor

progression and metastasis. Nat. Med. *19*, 1423–1437.

34. Suhail, Y., Cain, M.P., Vanaja, K., Kurywchak, P.A., Levchenko, A., Kalluri, R., and Kshitiz. (2019). Systems biology of cancer metastasis. Cell Syst. *9*, 109–127.

35. Lewis, M.T. (2000). Homeobox genes in mammary gland development and neoplasia. Breast Cancer Res. *2*, 158–169.

36. Maeda, K., Hamada, J.I., Takahashi, Y., Tada, M., Yamamoto, Y., Sugihara, T., and Moriuchi, T. (2005). Altered expressions of HOX genes in human cutaneous malignant melanoma. Int. J. Cancer *114*, 436–441.

37. Cheng, W., Liu, J., Yoshida, H., Rosen, D., and Naora, H. (2005). Lineage infidelity of epithelial ovarian cancers is controlled by HOX genes that specify regional identity in the reproductive tract. Nat. Med. *11*, 531–537.

38. Yu, Y.Y., Pan, Y.S., and Zhu, Z.G. (2007). Homeobox genes and their functions on development and neoplasm in gastrointestinal tract. Eur. J. Surg. Oncol. *33*, 129–132.

39. Wang, C., Shi, M., Ji, J., Cai, Q., Jiang, J., Zhang, H., Zhu, Z., and Zhang, J. (2019). A self-enforcing HOXA11/Stat3 feedback loop promotes stemness properties and peritoneal metastasis in gastric cancer cells. Theranostics *9*, 7628–7647.

40. Mimori, K., Shinden, Y., Eguchi, H., Sudo, T., and Sugimachi, K. (2013). Biological and molecular aspects of lymph node metastasis in gastro-intestinal cancer. Int. J. Clin. Oncol. *18*, 762–765.

41. Zhang, H., Wu, X., Xiao, Y., Wu, L., Peng, Y., Tang, W., Liu, G., Sun, Y., Wang, J., Zhu, H., et al. (2019). Coexpression of FOXK1 and vimentin promotes EMT, migration, and invasion in gastric cancer cells. J. Mol. Med. *97*, 163–176.

42. Sánchez-Tilló, E., Liu, Y., de Barrios, O., Siles, L., Fanlo, L., Cuatrecasas, M., Darling, D.S., Dean, D.C., Castells, A., and Postigo, A. (2012). EMT-activating transcription factors in cancer: beyond EMT and tumor invasiveness. Cell. Mol. Life Sci. *69*, 3429–3456.

43. Wu, Y.C., Tang, S.J., Sun, G.H., and Sun, K.H. (2016). CXCR7 mediates TGFβ1-promoted EMT and tumor-initiating features in lung cancer. Oncogene *35*, 2123–2132.

44. Sleeman, J., Schmid, A., and Thiele, W. (2009). Tumor lymphatics. Semin. Cancer Biol. *19*, 285–297.

45. Liu, S., Chen, X., and Lin, T. (2021). Lymphatic metastasis of bladder cancer: Molecular mechanisms, diagnosis and targeted therapy. Cancer Lett. *505*, 13–23.

46. Chen, C., He, W., Huang, J., Wang, B., Li, H., Cai, Q., Su, F., Bi, J., Liu, H., Zhang, B., et al. (2018). LNMAT1 promotes lymphatic metastasis of bladder cancer via CCL2 dependent macrophage recruitment. Nat. Commun. *9*, 3826.

47. Bushweller, J.H. (2019). Targeting transcription factors in cancer - from undruggable to reality. Nat. Rev. Cancer *19*, 611–624.

48. Li, Y., Azmi, A.S., and Mohammad, R.M. (2022). Deregulated transcription factors and poor clinical outcomes in cancer patients. Semin. Cancer Biol. *86*, 122–134.

STAR★METHODS

KEY RESOURCES TABLE

REAGENT or RESOURCE	SOURCE	IDENTIFIER
Antibodies		
HOXA11	Proteintech	Cat#55495-1-AP RRID:AB_2722488
Tubulin	Proteintech	Cat#11224-1-AP RRID:AB_2210206
E-Cadherin	Cell Signaling Technology	Cat#3195 RRID:AB_2291471
N-Cadherin	Cell Signaling Technology	Cat#13116 RRID:AB_2687616
Vimentin	Cell Signaling Technology	Cat#5741 RRID:AB_10695459
Snail	Cell Signaling Technology	Cat#3879 RRID:AB_2255011
Slug	Cell Signaling Technology	Cat#9585 RRID:AB_2239535
TGFβ-1	Proteintech	Cat#21898-1-AP RRID:AB_2811115
VEGF-C	Proteintech	Cat#22601-1-AP RRID:AB_2879132
Smad2	Proteintech	Cat#12570-1-AP RRID:AB_2193037
P-Smad2	Cell Signaling Technology	Cat#26945 RRID:AB_2798933
Pan-cytokeratin	Proteintech	Cat#26411-1-AP RRID:AB_2880505
LYVE-1	Affinity	Cat#AF4202 RRID:AB_2837586
Chemicals, peptides, and recombinant proteins		
D-Luciferin, Potassium Salt	Sciencelight	luc001
Matrigel matrix	Corning	356234
Disitertide (P144)	MedChemExpress	HY-P0118
Critical commercial assays		
CCK8	MedChemExpress	HY-K0301
24 mm Transwell® with 8.0 μm Pore Polycarbonate Membrane Insert	Corning	3428
SimpleChIP® Plus Enzymatic Chromatin IP Kit (Magnetic Beads)	Cell Signaling Technology	9005
Dual Luciferase Reporter Gene Assay Kit	Beyotime Biotechnology	RG027
Human VEGF-C ELISA Kit	Multisciences (Lianke) Biotechnology	EK1154
Deposited data		
Raw and analyzed data (RNA-seq)	This paper	Table S5; CNP0004514
Experimental models: Cell lines		
AGS	ATCC	CRL-1739

(*Continued on next page*)

Continued

REAGENT or RESOURCE	SOURCE	IDENTIFIER
SNU-216	ATCC	CRL-5974
MGC-803	Chinese Academy of Sciences	4201PAT-CCTCC01636
SGC-7901	Department of Pathology, Southern Medical University	N/A
Experimental models: Organisms/strains		
BALB/c Nude mice (female, 4-5 weeks old, 18-20 g)	Southern Medical University Laboratory Animal Centre (Guangzhou, China)	N/A
Oligonucleotides		
Primers for qPCR, see Table S3	MGH primerbank	https://pga.mgh.harvard.edu/primerbank/
si-HOXA11#1 Forward primer (5′-3′) GCGUCUACAUUAACAAAGATT	This paper	N/A
si-HOXA11#1 Reverse primer (5′-3′) UCUUUGUUAAUGUAGACGCTT	This paper	N/A
si-HOXA11#2 Forward primer (5′-3′) GAGACCGUUUACAGUACUATT	This paper	N/A
si-HOXA11#2 Reverse primer (5′-3′) UAGUACUGUAAACGGUCUCTT	This paper	N/A
si-HOXA11#3 Forward primer (5′-3′) GCAGUCUCGUCCAAUUUCUTT	This paper	N/A
si-HOXA11#3 Reverse primer (5′-3′) AGAAAUUGGACGAGACUGCTT	This paper	N/A
TGFβ1-P1 Forward primer (5′-3′) GATAGATAAGACGGTGGGAGC	This paper	N/A
TGFβ1-P1 Reverse primer (5′-3′) TGCTGATTCCCCACTCCCTGA	This paper	N/A
TGFβ1-P2 Forward primer (5′-3′) GGCATGGCACCGCTTCTGTCC	This paper	N/A
TGFβ1-P2 Reverse primer (5′-3′) CTGTCACTCAACACCCTGCGA	This paper	N/A
TGFβ1-P3 Forward primer (5′-3′) GCAGGGTGTTGAGTGACAGGA	This paper	N/A
TGFβ1-P3 Reverse primer (5′-3′) AGGATGGAAGGGTCAGGAGGC	This paper	N/A
VEGFC-P1 Forward primer (5′-3′) CTCCAGTTAGACCAGTTAAGC	This paper	N/A
VEGFC-P1 Reverse primer (5′-3′) AGTTTCCATTCAACCATTTGC	This paper	N/A
VEGFC-P2 Forward primer (5′-3′) AAGCAATAGAGAGATAGAAGG	This paper	N/A
VEGFC-P2 Reverse primer (5′-3′) TTGAAACTCCTCACCCATAAT	This paper	N/A
VEGFC-P3 Forward primer (5′-3′) GAAAGTCTCTTCTTCCGGTAA	This paper	N/A
VEGFC-P3 Reverse primer (5′-3′) GCAGGGTGAGCAGGTTACAGA	This paper	N/A
Software and algorithms		
ImageJ	National Institutes of Health	https://imagej.nih.gov/ij/
GraphPad Prism 9.0	GraphPad Prism Software, Inc	https://www.graphpad.com/
Adobe Illustrator CS6	Adobe	https://www.adobe.com/products/illustrator/

RESOURCE AVAILABILITY

Lead contact

Further information and requests for resources and reagents should be directed to and will be fulfilled by the lead contact, Yanfeng Hu (banby@smu.edu.cn).

Materials availability

This study did not generate new unique reagents and all materials in this study are commercially available.

Data and code availability

- Data: All data reported in this paper will be shared by the lead contact upon request. The data that support the findings of this study have been deposited into CNGB Sequence Archive (CNSA) of China National GeneBank DataBase (CNGBdb) with accession number CNP0004514, which is publicly accessible at https://db.cngb.org/. Relevant sequencing sample grouping information and RNA-seq tpm data are in Table S5.
- Code: This paper does not report original code.
- Additional information: Any additional information required to reanalyze the data reported in this paper is available from the lead contact upon reasonable request.

EXPERIMENTAL MODEL AND STUDY PARTICIPANT DETAILS

Patients and clinical specimens

A total of 80 formalin-fixed, paraffin-embedded gastric cancer specimens were collected from patients who underwent surgery at the Nanfang Hospital of Southern Medical University (Guangzhou, China) between December 2020 and December 2021. All samples were immediately snap-frozen in liquid nitrogen and stored at −80 °C until required. Two pathologists pathologically confirmed each sample by HE staining. Ethical consent was approved by the Committees for Ethical Review of Research involving Human Subjects at Southern Medical University. Written informed consent was obtained from each patient before sample collection. The clinical characteristics are summarized in Supplementary information, Table S2.

Cell lines and cell culture

The human gastric cancer cell lines AGS, SNU216, MGC803, BGC823 and SGC7901, and the normal gastric epithelial cell line GSE-1 were obtained from the Committee of the Typical Culture Collection of the Chinese Academy of Sciences and the Department of Pathology, Southern Medical University. All cells were cultured in RPMI1640 (Gibco, Shanghai, China). All media contained 10% fetal bovine serum, 100 U/ml penicillin and 100 μg/ml streptomycin. Human lymphatic endothelial cells (HLEC) were purchased from Science cells and cultured in endothelial cell culture medium (ECM; Science cells) containing 5% fetal bovine serum and endothelial cell growth medium (without vascular endothelial growth factor). All cells were cultured in an incubator with 5% CO2 at 37 °C.

Popliteal lymphatic metastasis model

BALB/c nude mice (female, 4-5 weeks old, 18-20 g) were purchased from the Southern Medical University Laboratory Animal Centre (Guangzhou, China). All experimental procedures were approved by the Institutional Animal Care and Use Committee of Southern Medical University. Mice were inoculated with 100 μl PBS gastric cancer cell suspension on their foot pads and these cells were transduced by HOXA11-luc, vector-luc, shHOXA11-luc or sh-NC-luc. After 4 weeks of rearing in the same environment, lymphatic metastases were monitored and imaged using a bioluminescence imaging system (PerkinElmer, IVIS Spectrum Imaging System). The primary tumour and popliteal lymph nodes were then excised and photographed for documentation. Paraffin embedding and sectioning were then processed for comparative analysis of tumour growth and lymphatic metastases by IHC.

METHOD DETAILS

siRNA and lentiviral transduction

siRNAs targeting HOXA11 were designed and synthesized by GenePharma (Suzhou, China) (sequences listed in Table S3). The two siRNAs with the best knockdown efficiency were used in the subsequent functional studies.

HOXA11 overexpression lentiviral plasmids were constructed by Genechem (Shanghai, China). For lentiviral transduction, the packaging plasmid and HOXA11 overexpression vector or control vector were co-transfected and the virus-containing supernatant was collected, followed by transfection of the lentiviral vector into the target cells. The transduced gastric cancer cells were subsequently screened with 3 μg/ml puromycin.

Quantitative Real Time PCR (qRT-PCR)

For qRT-PCR experiments, RNA was extracted from all gastric cancer cell lines and GC tissues to be tested using the Eastep® Super Total RNA Extraction Kit (Promega, USA). cDNA was reverse transcribed from the extracted RNA using the PrimeScript™ RT Master Mix (Takara, Japan). qRT-PCR experimental reactions were performed using Hieff™ qPCR SYBR Green Master Mix (Yessen, China). Relative mRNA quantification was calculated using the $2^{-\Delta\Delta Ct}$ method and GAPDH was used as the standard. All primer sequences used for qRT-PCR are shown in the Table S3. All experiments were performed in triplicate.

Western blot analysis

Briefly, the proteins of the gastric cancer cells and tissues to be tested were extracted using RIPA buffer (Beyotime Biotechnology, China). The protein samples were separated electrophoretically by SDS-PAGE gels (7.5-12%) and then transferred to PVDF membranes. After a blocking treatment in 5% skimmed milk, the membranes were incubated with primary antibodies overnight at 4°C and then incubated with specific secondary antibodies for one hour at room temperature. Finally the expression of the target protein was detected using an ECL kit (Millipore, USA). The primary antibodies used for Western blot are listed in Table S4.

Immunohistochemical (IHC) staining

Immunohistochemistry (IHC) assays are performed on specimen tissues from gastric cancer patients, mouse tumour tissues and lymph node tissues. The primary antibodies used in immunohistochemistry include: HOXA11, human pancytokeratin, and LYVE-1 lymphovascular marker protein. The primary antibodies used for IHC are listed in Table S4. Immunohistochemistry results are scored by classifying the intensity of staining according to the level of expression of the target protein (0=negative, 1=weak, 2=moderate, 3=strong) and the area of staining (0=0%, 1=1-25%, 2=26-50%, 3=51-100%).

CCK-8 assay

Cell proliferation was dynamically assessed using the Cell Counting Kit CCK-8 assay (MedChemExpress; HY-K0301). 1000 cells were seeded in each well of a 96-well plate, with three replicate wells designed for each group to be assayed. Then, at a fixed time point each day, 10 μl of CCK-8 solution was added and incubated at 37°C for one hour. The absorbance was measured at 450 nM using an automated microplate reader.

Colony-forming assay

For the colony formation assay, gastric cancer cell lines from different treatment groups were added to 6-well plates at 500 cells/well. These plates were then incubated in serum-free RPMI-1640 for 14 days. The plates were subsequently stained with crystalline violet. After the stained plates were photographed and recorded, the number of colonies in each group was calculated from the images. Each experimental treatment was performed three times.

Cell scratch wound-healing assay

Gastric cancer cells from the different treatment groups were first cultured in six-well plates until they were fully confluent. A suitable micropipette tip was then used to produce a uniform scratch from the centre of each well. After washing with phosphate-buffered saline (PBS), the cells were cultured in medium without fetal bovine serum (FBS) and photographed at 0 hours and at a fixed time point each day thereafter. The rate of cell migration was measured by comparing the change in gap between groups of cells.

Cell transwell migration and invasion assays

Transwell chambers (Corning, USA) with a pore size of 8.0 μm were used for cell migration and invasion assays. Cells (1×10^4/well) in 200 μL of serum-free medium were seeded into the upper chamber, and 600 μL of medium containing 10% FBS or different treatment groups were added to the lower layer. The upper

compartment of the transwell was coated with Matrigel (BD Bioscience, USA) for the invasion assay or left uncoated for the migration assay. Cells that migrated or invaded into the lower chamber were subsequently stained with 0.1% crystal violet at the 24 or 36 hour time points, respectively, and then photographed for documentation and count analysis. Each experiment was performed independently in triplicate.

HLECs tube formation assay

Supernatant cultures of gastric cancer cells from the different treatment groups were collected. HLECs were inoculated into Ibidi angiogenesis slides (pre-coated Matrigel) containing this supernatant culture and incubated in a cell warmer for 4 hours, followed by photography of lymphatic tube generation under an inverted microscope. Quantitative comparisons were also made by measuring the length of intact tubular structures in the different treatment groups.

ELISA assay

VEGF-C concentrations in cell culture supernatants with different HOXA11 expression levels were quantified and compared using the VEGF-C ELISA kit (UNI, China) according to the instructions. All sample experiments were repeated in triplicate.

Cellular immunofluorescence assay

Cells were seeded on confocal discs (Cellvis, USA) for 24 hours prior to fixation with paraformaldehyde and permeabilisation with Triton X-100. After blocking with 5% normal donkey serum, cells were incubated overnight at 4°C with primary antibodies specific for E-cadherin (1:200, CST), N-cadherin (1:200, CST), Vimentin (1:100, CST) and Smad2 (1:400, CST), followed by incubation with fluorescence-conjugated secondary antibodies at room temperature for 1 hours. Cells were then counterstained with DAPI (Sigma, Germany) and photographed with a confocal laser scanning microscope (Leica, Germany).

Chromatin immunoprecipitation (ChIP)

ChIP assays are performed using the SimpleChIP® Plus Enzymatic Chromatin IP Kit (Magnetic Beads) (CST, USA), protocol according to instructions. For the ChIP-qPCR assay, primers explicitly designed to target the TGFβ1 or VEGF-C promoter region were listed in Table S3.

Dual-luciferase reporter gene assay

For the dual luciferase reporter assay, HOXA11 overexpression plasmids, pGL3-TGFβ1 (TGFβ1-WT) and pGL3-mutated TGFβ1 (TGFβ1-mut) plasmids were constructed and synthesised by Genechem (Shanghai, China). SNU216 and MGC803 cells were cotransfected with luciferase reporter plasmids using Lipofectamine 3000 (Invitrogen, USA) and 48 hr post-transfection luciferase assays were performed using the Dual Luciferase Reporter System kit (Beyotime, China). All assays were performed in triplicate.

QUANTIFICATION AND STATISTICAL ANALYSIS

All quantitative data are presented as the mean ± standard deviation from at least three independent experiments. The chi-square test ($\chi 2$ test) for non-parametric variables and Student's t-test or one-way analysis of variance (ANOVA) for parametric variables (two-tailed tests) were used to identify statistically significant data. All statistical analyses were conducted using SPSS v21.0 and p-values < 0.05 were considered statistically significant.